

Effect of Sn/Zn/Cu precursor stack thickness on two-step processed kesterite solar cells

Peer-reviewed author version

Ranjbar, Samaneh; BRAMMERTZ, Guy; VERMANG, Bart; Hadipour, Afshin; Sylvester, M.; Mule, Aniket; MEURIS, Marc; da Cunha, A. F. & POORTMANS, Jef (2017) Effect of Sn/Zn/Cu precursor stack thickness on two-step processed kesterite solar cells. In: THIN SOLID FILMS, 633(SI), p. 127-130.

DOI: 10.1016/j.tsf.2016.09.040

Handle: <http://hdl.handle.net/1942/24410>

# Effect of Sn/Zn/Cu precursor stack thickness on two-step processed kesterite solar cells

Samaneh Ranjbar <sup>1,4,5\*</sup> , Guy Brammertz <sup>2,3</sup> , Bart Vermang <sup>2,3,4</sup> , Afshin Hadipour <sup>4</sup> , M. Sylvester <sup>2,4,5</sup> , Aniket Mule<sup>4,5,6</sup> , Marc Meuris <sup>2,3</sup> , A. F. da Cunha<sup>1</sup> and Jef Poortmans <sup>3,4,5</sup>

<sup>1</sup> I3N - Departamento de Física, Universidade de Aveiro, Campus Universitário de Santiago, 3810-193 Aveiro, Portugal.

<sup>2</sup> imec division IMOMEC - partner in Solliance, Wetenschapspark 1, 3590 Diepenbeek, Belgium

<sup>3</sup> Institute for Material Research (IMO) Hasselt University, Wetenschapspark 1, 3590 Diepenbeek, Belgium

<sup>4</sup> imec- partner in Solliance, Kapeldreef 75, 3001 Leuven, Belgium

<sup>5</sup> Department of Electrical Engineering (ESAT), KU Leuven, Kasteelpark Arenberg 10, 3001 Heverlee, Belgium

<sup>6</sup> Department of Mechanical and Process Engineering (D-MAVT), ETH Zurich, LEE K, Leonhardstrasse 21, 8092 Zurich, Switzerland

**Key:** RCJI6

---

\* Corresponding author; Tel: [+351 234370818](tel:+351234370818); E-mail: [samaneh.ranjbar@ua.pt](mailto:samaneh.ranjbar@ua.pt)

## **Abstract**

The effect of variation of thickness of  $\text{Cu}_2\text{ZnSnSe}_4$  (CZTSe) absorber layers on physical and optoelectronic properties of CZTSe/CdS/ZnO solar cells has been investigated. CZTSe absorber layers with different thickness were fabricated by selenization of e-beam evaporated Sn, Zn and Cu layers. Scanning electron microscopy revealed that by increasing the thickness the morphology of CZTSe films improves substantially and energy dispersive spectrometry measurements showed that the Cu to Sn ratio increased with increasing film thickness, despite a similar Cu to Sn ratio in the starting layer. A longer minority carrier lifetime and higher open circuit voltage were achieved for solar cells with thicker absorber layers. A maximum conversion efficiency of 7.8 % was achieved for a solar cell with 1.7  $\mu\text{m}$  thickness in which a low doping density of the order of  $10^{15} \text{ cm}^{-3}$  was measured, leading to a wide space charge region of about 300 nm.

## **Keywords:**

CZTSe solar cell, absorber layer thickness, minority carrier lifetime, space charge region.

## **1. Introduction**

Kesterite compound  $\text{Cu}_2\text{ZnSn}(\text{S},\text{Se})_4$ , CZTSSe is being investigated as a promising candidate for cost effective thin film solar cells. In addition of desirable photovoltaic properties such as high absorption coefficient ( $> 10^4 \text{ cm}^{-1}$ ) and optimal band gap (1 - 1.5 eV depending on the S/Se composition ratio), CZTSSe consists of inexpensive and abundant elements [1]. So far 12.6 % conversion efficiency has been achieved for a CZTSSe solar cell synthesized by a hydrazine solution based process [2]. The effect of variation of thickness of absorber layer has been studied

for pure sulfide  $\text{Cu}_2\text{ZnSnS}_4$  [3]. We fabricated pure selenide  $\text{Cu}_2\text{ZnSnSe}_4$  films by selenization of e-beam evaporated Sn, Zn and Cu layers. The effect of variation of thickness of the absorber layers on the physical, optical and electrical properties of the solar cell devices is investigated.

## 2. Experimental details

Pure  $\text{Cu}_2\text{ZnSnSe}_4$  (CZTSSe) absorber layers were synthesized in a two-step process. First, Sn, Zn and Cu were subsequently deposited on Mo-coated Soda Lime Glass, (SLG) by e-beam evaporation. Metallic layers with different thickness (See Table.1) were deposited while the metallic ratios were kept constant in order to control the composition. In the second step, the Sn/Zn/Cu stacks were selenized by 10%  $\text{H}_2\text{Se}$  gas diluted in  $\text{N}_2$  for 15 min at 460 °C in a rapid thermal processing system with 1 °C/s heating rate. This selenization process has been already optimized and applied for sputtered  $\text{Cu}_{10}\text{Sn}_{90}/\text{Zn}/\text{Cu}$  stack layers [4]. Absorber layers with thicknesses of ~ 300, 700, 1000, 1200 and 1700 nm were fabricated. These absorber layers were etched in 5 % KCN solution for 2 min to remove the secondary phases from the surface. Solar cells were then completed by successive chemical bath deposition of CdS (~ 50 nm ), sputtering of intrinsic ZnO (~ 50 nm ) and Al-doped ZnO (~ 300-400 nm ) and finally evaporation of Ni/Al grids. Solar cells with 0.5 cm<sup>2</sup> area were isolated by needle scribing of the devices. Scanning electron microscopy (SEM) and energy dispersive spectrometry (EDS) of the absorbers were acquired by SU-70 Hitachi combined with a Rontec EDS system, at acceleration voltages of 5 kV. The thickness of the samples are measured by cross sectional SEM images. The electrical characterization of the solar cells were studied by light and dark current–voltage (I–V) using an Oriel solar simulator system with an AM1.5 G spectrum and 1 sun illumination. Capacitance–Voltage (C–V) were measured with an Agilent 4980A LCR-meter as a function of frequency varying from 10 kHz to 100 kHz and bias voltage from – 2 V to 0.5 V, while AC voltage was 30

mV. Room temperature TRPL measurement were acquired by a Hamamatsu C12132. An area of 3 mm diameter of completed solar cells were illuminated by a 532 nm laser with 15 kHz repetition rate and 1.0 mW average power.

### **3. Results and discussion**

#### *3.1 Morphological analysis*

Top-view SEM images of CZTSe absorber layers with different thickness are shown in [Fig.1.a](#) to [Fig.1.d](#) and cross-sectional SEM images of devices with 700 nm and 1700 nm thickness are shown in [Fig.1.e](#) and [Fig.1.f](#), respectively. SEM images reveal that by increasing the thickness the morphology of the absorbers improves, the grain size increases and less voids and pinholes can be observed in the films.

The composition of the samples was measured by EDS and the results are given in Table 1. Although the metallic ratios were kept constant in order to control the composition and X-ray fluorescence measurement of initial precursors confirmed the expected thicknesses for all samples, the Cu/Sn decreases constantly by decreasing the thickness. The reason of Sn excess composition of the thinner samples is not quite clear, however, the faster interdiffusion of the three metal layers and consequently reduced formation of volatile SnSe<sub>2</sub> might be the reason for larger amount of Sn in the thinner samples as compared to the thicker samples.

#### *3.2 Optical and electrical characterization:*

[Fig.2 \(a\)](#) shows the room temperature photoluminescence (PL) of the solar cells. The position of the PL peak of the solar cells with different thickness is summarized in Table.2. By decreasing the thickness, the PL spectra become broader and the PL peak position shifts slightly towards lower energies. The PL peak of CZTSe is generally attributed to a donor to acceptor recombination in

the presence of a large amount of band tail states and potential fluctuations [5]. The red shift of the PL spectra by decreasing the thickness might be due to a larger amount of band tail states in the thinner samples. The reason of larger tailing states in thinner samples is not completely clear but it can be due to several reasons such as the Sn rich composition which can lead to formation of  $\text{Sn}_{\text{Cu}}$  and  $\text{Sn}_{\text{Zn}}$  deep donors, or the formation of secondary phases with different band gaps that produce band tailings.

[Fig.2 \(b\)](#) shows the minority carrier lifetime,  $\tau$  of solar cells with different thickness. The minority carrier lifetime is derived using a two exponential fit to the photoluminescence decay curve. The slower decay time usually is considered as the minority carrier lifetime [6]. The lifetime of the samples increases by increasing the thickness and it reaches 8.4 ns when thickness of absorber layer is 1700 nm. The enhancement of the lifetime by increasing the thickness is correlated to the lower doping concentration ([See. Fig.4](#)). Also the Sn rich composition of ultra thin samples may lead to electron trapping defects such as  $\text{Sn}_{\text{Cu}}$ ,  $\text{Sn}_{\text{Zn}}$  or other compensated defect clusters that increase the recombination and degrade the minority carrier lifetime significantly.

[Fig.3](#) shows the illuminated / dark J-V curve (solid/dashed lines) of the champion solar cells of each thickness. The corresponding cell parameters are derived from the procedure explained in [Ref.7](#) and are summarized in [Table.2](#). Shunt resistance,  $R_{\text{sh}}$  is very low when the absorber thickness is  $\leq 1000$  nm and it improves significantly to  $512 \Omega \cdot \text{cm}^2$  for the thickest sample since the film becomes more compact.  $J_{\text{sc}}$  is very low when the thickness of the device is  $\leq 1000$  nm because of the incomplete collection of solar spectrum. Further improvement of  $J_{\text{sc}}$  of samples thicker than 1000 nm can be attributed to a wider Space Charge Region (SCR) that facilitate the collection of carriers. [Fig.6 \(c\)](#) shows that by increasing the thickness from 1000 nm to 1700 nm the SCR increases from 70 nm to 300 nm and  $J_{\text{sc}}$  improves up to  $36.4 \text{ mA/cm}^2$ . The significant improvement

of  $V_{oc}$  by increasing the thickness indicates the reduction of recombination currents and it is consistent with the enhancement of minority carrier lifetime (See Fig.6 (b)). The recombination in CZTSe is mainly attributed to the recombination in SCR [8], however, the dramatic decrease of  $V_{oc}$  in ultra thin samples might be also due to the contribution of rear interface recombination because of the decomposition of CZTSe near the Mo surface [9].

Fig.4 shows the doping density profile of absorbers with different thicknesses obtained by Mott–Schottky plot from the C-V measurement at frequency of 40 kHz. By increasing the thickness, the doping density at the edge of SCR,  $N_a$ , decreases substantially, thus the SCR becomes wider. The reason for this large variation in doping density is not quite clear but might also be related to the large variation of the Cu to Sn ratio in the absorbers with different thickness. As Fig.6 (a) shows by increasing the thickness the Cu to Sn ratio increases while the doping density decreases significantly.

Finally, the EQE measurement shown in Fig.5 indicates that by increasing the thickness photocurrent collection improves mainly due to the wider SCR and longer lifetime.

#### **4. Conclusions:**

In conclusion, increasing the thickness improved the quality of CZTSe absorber layers prepared by selenization of e-beam evaporated Sn/Zn/Cu stacks. Thicker metal starting layers led to a larger Cu to Sn ratio in the final absorber, possibly because the thinner starting layers show faster interdiffusion of the metals and suppressed SnSe<sub>2</sub> evaporation. The enhanced physical quality of the absorber layers leads to higher performance of solar cells, especially due to a, longer minority carrier lifetime and accordingly higher  $V_{oc}$  . In

addition, it was found that the doping of the absorber layer increased with decreasing sample thickness and the wider space charge region of thicker devices lead to better collection of photogenerated carriers and higher  $J_{sc}$ .

## Acknowledgements

This project has received funding from the European Union's Horizon 2020 research and innovation program under grant agreement No 640868. This research is partially funded by the Flemish government, Department Economy, Science and innovation. Samaneh Ranjbar acknowledge the financial support of the Portuguese Science and Technology Foundation (FCT) through PhD grant SFRH / BD / 78409 / 2011.

## References

- [1] Kentaro ITO, Copper Zinc Tin Sulfide-Based Thin-Film Solar Cells, WILEY, 2014.
- [2] W. Wang, M.T. Winkler, O. Gunawan, T. Gokmen, T.K. Todorov, Y. Zhu, D.B. Mitzi, Device characteristics of CZTSSe thin-film solar cells with 12.6% efficiency, *Adv. Energy Mater.* 4 (2014) 1301465–1301469.
- [3] Ren, Y., Scragg, J. J. S., Frisk, C., Larsen, J. K., Li, S.-Y. and Platzer-Björkman, Influence of the  $\text{Cu}_2\text{ZnSnS}_4$  absorber thickness on thin film solar cells, *Phys. Status Solidi A* 212, (2015) 2889–2896.
- [4] G. Brammertz, M. Buffière, Oueslati, H. ElAnzeery, K. Ben Messaoud, S. Sahayaraj, C. Koble, M. Meuris, and J. Poortmans, Characterization of defects in 9.7% efficient  $\text{Cu}_2\text{ZnSnSe}_4\text{-CdS-ZnO}$  solar cells, *Appl. Phys. Lett.* 103 (2013) 163904-163907.
- [5] Souhaib Oueslati, Guy Brammertz, Marie Buffière, Christine Köble, Touayar Oualid, Marc Meuris, Jef Poortmans, Photoluminescence study and observation of unusual optical



- transitions in  $\text{Cu}_2\text{ZnSnSe}_4/\text{CdS}/\text{ZnO}$  solar cells, *sol. Energy mater. and sol. Cells*, 134 (2015) 340-345.
- [6] A. Kanevce, D. H. Levi and D. Kuciauskas, The role of drift, diffusion, and recombination in time resolved photoluminescence of CdTe solar cells determined through numerical simulation, *Prog. Photovolt: Res. Appl.* 22, (2014) 1138–1146.
- [7] Hegedus, S. S. and Shafarman, W. N., Thin-film solar cells: device measurements and analysis. *Prog. Photovolt: Res. Appl.* 12 (2004) 155–176
- [8] Guy Brammertz, Souhaib Oueslati, Marie Buffiere, Jonas Bekaert, Hossam El Anzeery, Khaled Ben Messaoud, Sylvester Sahayaraj, Thomas Nuytten, Christine K'oble, Marc Meuris, and Jozef Poortmans, Investigation of Properties Limiting Efficiency in  $\text{Cu}_2\text{ZnSnSe}_4$ -Based Solar Cells, *IEEE j. of photovolt.* 5 (2015) 649-655.
- [9] Jonathan J. Scragg, J. Timo Wätjen, Marika Edoff, Tove Ericson, Tomas Kubart, and Charlotte Platzer-Björkman, A Detrimental Reaction at the Molybdenum Back Contact in  $\text{Cu}_2\text{ZnSn}(\text{S},\text{Se})_4$  Thin-Film Solar Cells, *j. of the American Chemical Society* 134 (2012) 19330-19333.

Table 1. Metal composition of CZTSe absorbers with different thickness.

<b>Thickness (nm)</b>	<b>Thickness (nm)</b>	<b>Cu</b>	<b>Cu</b>	<b>Zn</b>	<b>Cu</b>
<b>Sn/Zn/Cu</b>	<b>After Selenization</b>	<b>Zn</b>	<b>Sn</b>	<b>Sn</b>	<b>Sn+Zn</b>
54/26/30	300	1.97	1.24	0.63	0.76
107/53/60	730	1.34	1.38	1.03	0.68
215/105/120	1000	1.51	1.59	1.06	0.77

260/126/145	1200	1.49	1.59	1.07	0.77
310/150/160	1700	1.71	1.74	1.04	0.86

Table 2. Electrical and optical parameters of solar cells with different absorber thickness: short circuit current ( $J_{sc}$ ), open circuit voltage ( $V_{oc}$ ), fill factor (FF), efficiency ( $\eta$ ), shunt resistance ( $R_{sh}$ ) and series resistance ( $R_s$ ) are derived from illuminated current-voltage (J-V) measurement,  $J_{sc}$  (EQE) are derived from external quantum efficiency (EQE). PL peak position (PL) and lifetime ( $\tau$ ) are derived from time resolved photoluminescence measurement.

Thickness (nm)	$J_{sc}$ (mA/cm <sup>2</sup> )	$J_{sc}$ (EQE) (mA/cm <sup>2</sup> )	$V_{oc}$ (mV)	FF (%)	$\eta$ (%)	$R_{sh}$ ( $\Omega$ .cm <sup>2</sup> )	$R_s$ ( $\Omega$ .cm <sup>2</sup> )	PL (eV)	$\tau$ (ns)
300	2.3	–	175.0	25	0.1	68	2.07	0.89	0.1
730	15.2	–	262.0	34	1.4	31	1.16	0.89	1.4
1000	26.9	26.60	363.0	47	4.6	98	1	0.93	5.3
1200	30	34.92	385.0	54	6.2	277	1.26	0.91	6.8
1700	36.4	39.50	406.0	53	7.8	512	1.35	0.95	8.4

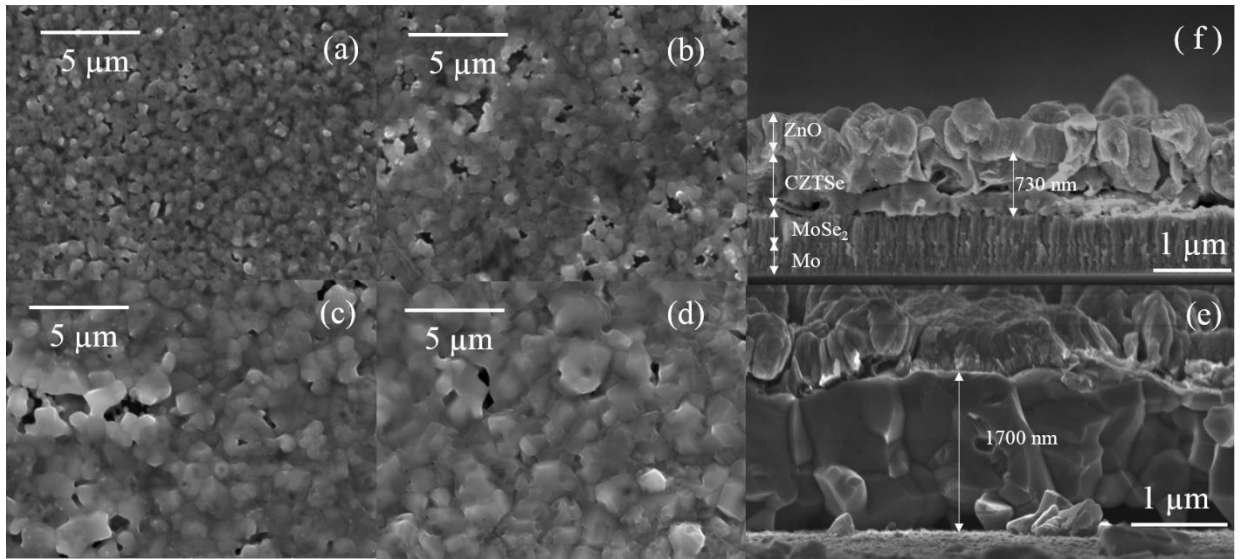


Fig.1. Top view SEM images of absorber layers: (a) to (d) absorbers with 300, 700, 1200,1700 nm thickness.(e) and (f) Cross section SEM images of solar cells with absorber layer thickness of 700 nm and 1700 nm.

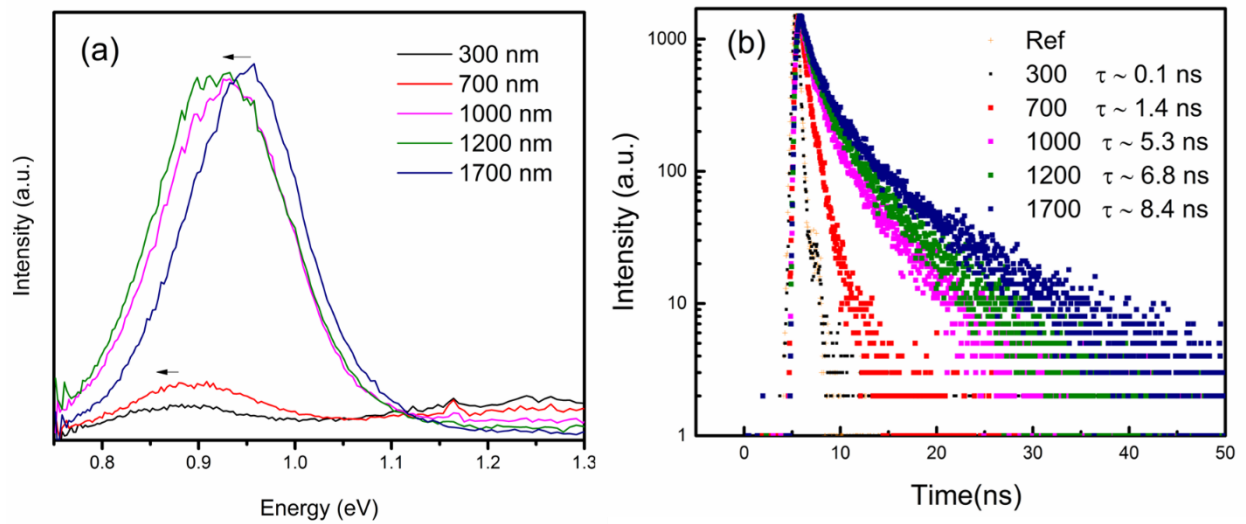


Fig.2. (a) Photoluminescence spectra and (b) time resolved Photoluminescence spectra of solar cells with different absorber thickness. Minority carrier lifetime ( $\tau$ ) is derived form a two exponential fit.

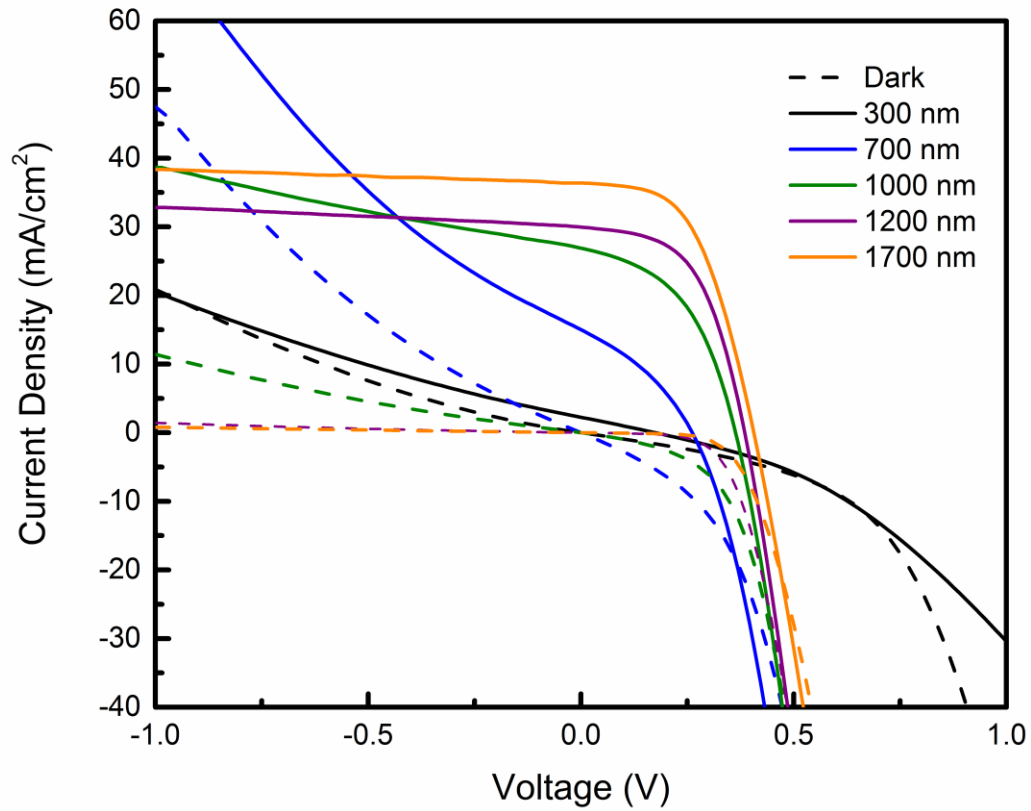


Fig.3. Current-Voltage measurement of solar cells with different absorber thickness under dark (dashed line) and 1 sun illumination (solid line).

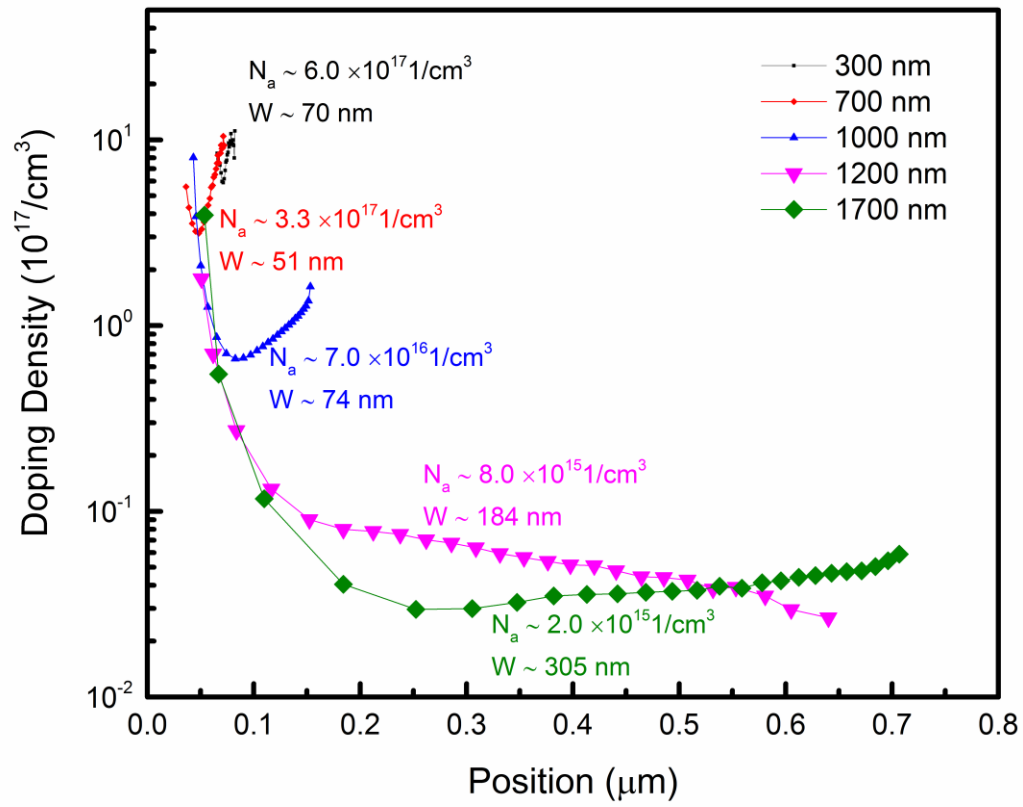


Fig.4. Doping density profile of solar cells with different absorber thickness. The hole concentration ( $N_a$ ) and space charge region width ( $W$ ) are derived from Mott-Schottky plot.

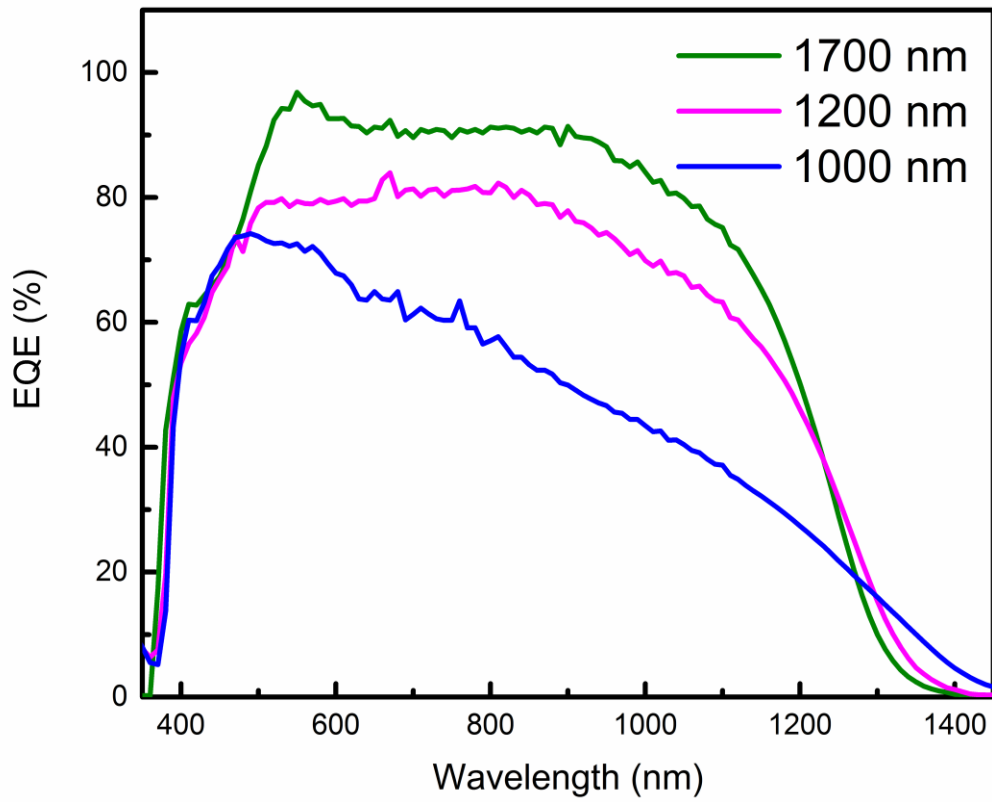


Fig.5. External quantum efficiency (EQE) of solar cells with different absorber layer thickness.

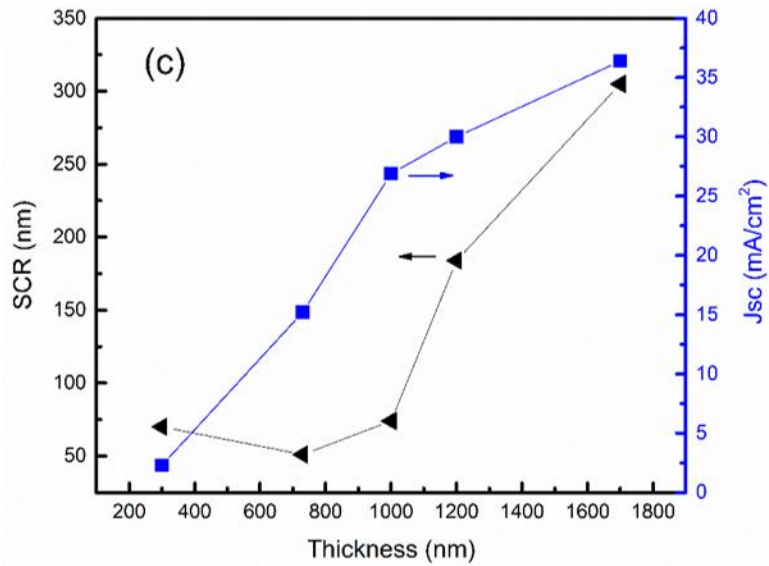
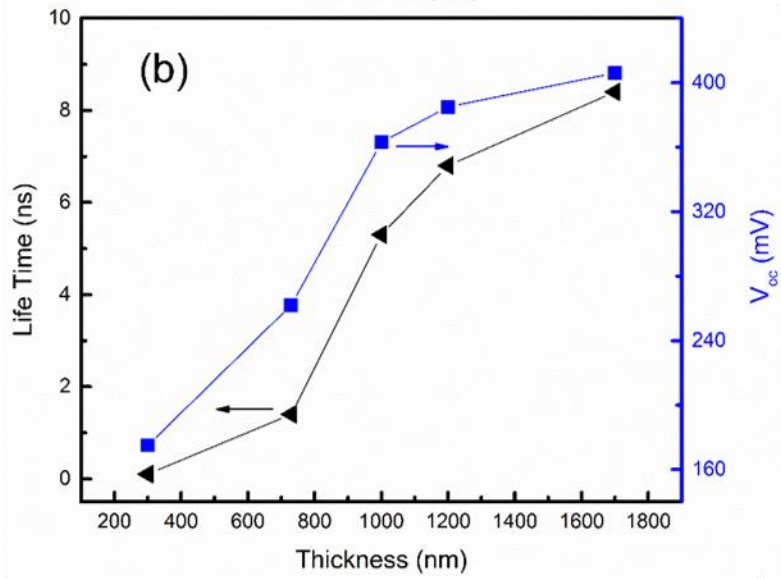
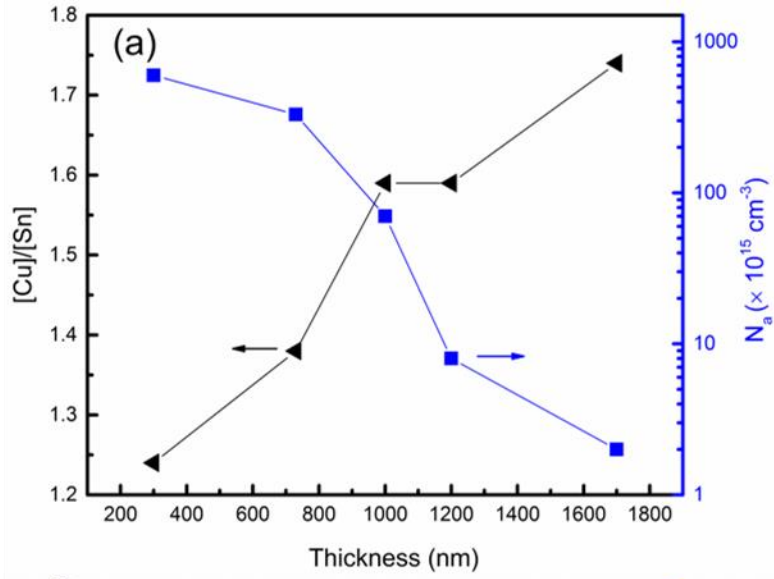


Fig.6. (a) Cu to Sn ratio and hole concentration,  $N_a$ , (b) Minority carrier lifetime and  $V_{oc}$ , (c) Depletion width (SCR) and  $J_{sc}$  at various thickness.